

# Microscopic Description of Induced Fission

**Nicolas Schunck**

Physics Division, Lawrence Livermore National Laboratory, CA 94551, USA

E-mail: [schunck1@llnl.gov](mailto:schunck1@llnl.gov)

**Abstract.** Selected aspects of the description of neutron-induced fission in  $^{240}\text{Pu}$  in the framework of the nuclear energy density functional theory at finite temperature are presented. In particular, we discuss aspects pertaining to the choice of thermodynamic state variables, the evolution of fission barriers as function of the incident neutron energy, and the temperatures of the fission fragments.

## 1. Introduction

Nuclear fission remains one of the most complex physics phenomena in nature. Powerful phenomenological models, finely tuned to a wealth of precise experimental data, have given us a good qualitative, and at times quantitative, understanding of the phenomenon. However, these models of fission lack a firm connection with the theory of the nuclear force. This jeopardizes their ability to supply the high-precision predictions currently needed to understand the later stages of the formation of elements in supernova, or to simulate new prototypes of nuclear reactors.

Some of the basic concepts of a microscopic theory of fission were already laid out in the eighties by the theory group at CEA Bruyères-le-Châtel in France [1, 2]. Starting from an effective interaction between nucleons that embeds (in a phenomenological way) in-medium many-body correlations, the nuclear self-consistent mean-field theory provides a generic framework to construct ever more accurate representations of the nuclear wavefunction [3]. To describe fission, a number of collective variables must be introduced. The potential energy surface in the collective space thus defined serves as a basis to perform a time evolution of the nuclear wave packet in the framework of the time-dependent generator coordinate method. As evidenced from the few applications reported, the method is very promising [4].

However, at the time of its inception, the necessary computing power was lacking so that this approach could not yet compete with more empirical models. Today, the fast development of leadership class computers and interdisciplinary collaborations such as the NUCLEI project open new perspective [5]. In addition, recent progress in deriving quality energy functionals for fission applications [6] and of understanding the quantum mechanics of scission [7] suggests the microscopic approach to fission has enough potential to become predictive.

In this work, we discuss some aspects of the microscopic theory of fission in the poster-child example of the neutron-induced fission of  $^{240}\text{Pu}$  at low energies. After a brief reminder of the theoretical framework, we show the evolution of the fission barriers as function of the nuclear temperature, and discuss some of the practical aspects related to such simulations.

## 2. Theoretical framework

Our formalism is based on the nuclear energy density functional theory (DFT) with local energy functionals of the Skyrme type [8] for the particle-hole channel, and contact density-dependent interactions with mixed volume and surface character for the particle-particle channel [9]. The nucleus is described at the Hartree-Fock-Bogoliubov approximation: its ground state is a quasi-particle vacuum that depends on a number of collective variables  $\mathbf{q} = \{q_i\}_{i=1,\dots,N}$ , such as, e.g. the expectation value of multipole moments or angular momentum. The set of the  $N$  collective variables defines a point  $\mathbf{q}$  in the collective space. For each point in the collective space, the requirement that the energy be minimal with respect to variations of the generalized density leads to the HFB equations; solving the latter defines the one-body density matrix and the pairing tensor, and thereby all observables of interest.

The finite-temperature extension of the HFB formalism (FT-HFB) was introduced in nuclear physics more than 30 years ago [10]. We only recall that in the finite-temperature HFB theory, the ground-state is a statistical superposition of pure quantum states, characterized by a density operator  $\hat{D}$ . Adopting the HFB approximation for the density operator leads to the finite-temperature HFB equations: they are formally equivalent to their form at zero-temperature, only the expression of the density matrix and pairing tensor is different. Most importantly, the Wick theorem still applies, meaning that all observables are computed from the trace (in the given representation) of the corresponding operator and the one-body density matrix.

In addition to the density operator, macroscopic thermodynamical concepts are also used to describe the system at finite temperature. In particular, several thermodynamical potentials are available to describe the nucleus, each coming with its set of state variables. The two most useful are (i) the internal energy  $E(V, S, X)$ , where  $V$  is the (constant) nuclear volume,  $S$  the entropy and  $X$  any additional extensive state variable needed to characterize the nucleus (expectation value of multipole moment, for example) and (ii) the Helmholtz free energy  $F(V, T, X)$  with  $F = E - TS$  and  $T$  the temperature. The FT-HFB equations are obtained by minimization of the grand potential at temperature  $T$ , and naturally yield the free energy in the isothermal representation (constant  $T$ ). Passage to an isentropic description (constant  $S$ ) is sometimes needed, as discussed below.

## 3. Induced fission and finite-temperature formalism

In the description of induced fission in the finite-temperature DFT framework, the first step is to compute the potential energy surface of the nucleus as a function of the chosen collective coordinates and the nuclear temperature. In the following, we work in a four-dimensional collective space characterized by the expectation values of the axial,  $\hat{Q}_{20}$ , and triaxial,  $\hat{Q}_{22}$ , quadrupole moment, mass octupole moment  $\hat{Q}_{30}$  and hexadecapole moment  $\hat{Q}_{40}$ . All calculations have been performed with the SkM\* parametrization of the Skyrme functional [11]. In the particle-particle channel, the proton and neutron pairing strengths were fitted to the experimental 3-point formula for the odd-even mass differences in  $^{240}\text{Pu}$ . A cutoff of  $E_{\text{cut}} = 60$  MeV limits the number of quasi-particles taken into account in the calculation of the densities.

Calculations were performed with the DFT solvers HFBTHO [12] and HFODD [13]. In both codes the solutions to the HFB equations are expanded in the one-center harmonic oscillator (HO) basis. In HFBTHO axial and time-reversal symmetry are assumed so that solutions are labeled by the projection of the angular momentum on the  $z$ -axis. By contrast, HFODD is fully symmetry-unrestricted, and can, in particular, describe triaxial and parity-breaking shapes. The two programs have been benchmarked against one another and agree within a few eV for an axial configuration [12]. In practice, the HFB wavefunctions were expanded onto  $N_{\text{states}} = 1100$  HO basis states with contributions from up to  $N_{\text{max}} = 30$  oscillator shells.

### 3.1. Evolution of fission barriers

In figure 1, we show the evolution of the free energy  $F = E - TS$  as function of the expectation value  $Q_{20}$  of the axial quadrupole moment. All three other degrees of freedom are locally minimized: in practice, the first barrier has a non-zero value of  $\hat{Q}_{22}$  while the octupole moment is non-zero past the second barrier. Note the gradual disappearance of the barriers as the temperatures increases.

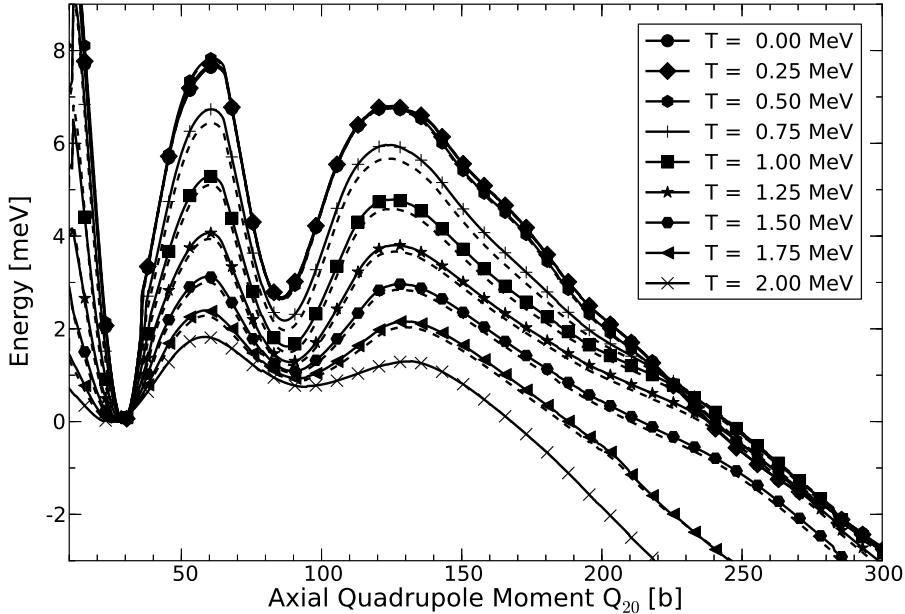


**Figure 1.** Evolution of fission barriers in  $^{240}\text{Pu}$  as a function of temperature along the most probable fission path. Plain lines curves with a symbol show the free energy at constant temperature (isothermal process), the dashed-line curves next to them show the corresponding internal energy at constant entropy (isentropic process).

In applications of induced fission, the primary motivation has to do with the properties of the fission fragments rather than those of the fissioning compound nucleus. Of particular importance are the charge and mass distributions of the fragments, their total kinetic energy (TKE), and their excitation energy. The latter is a major input in the reaction codes that model the neutron and gamma spectrum generated during fission. Estimates of TKE and excitation energy require, in principle, to work in the isentropic representation. The Maxwell relations of thermodynamics state that, for any (extensive) collective coordinate  $q_i$ ,

$$\left. \frac{\partial F}{\partial q_i} \right|_{T, q_j \neq i} = \left. \frac{\partial E}{\partial q_i} \right|_{S, q_j \neq i}. \quad (1)$$

Therefore, variations of internal energy with respect to deformation at constant entropy are equal to the variations of free energy at constant temperature [14].

From the set of curves  $\{F(\mathbf{q}, T_k)\}_k$  obtained directly from the FT-HFB calculations, one can, by numerical interpolation, reconstruct the  $E(\mathbf{q}, S)$  for any value  $S$  of the entropy. The procedure is based on a standard spline interpolation. Finite-temperature HFB calculations

produce at each point  $\mathbf{q}$  in the collective space the quantities  $E(T)|_{\mathbf{q}}$  and  $S(T)|_{\mathbf{q}}$ , where from we easily obtain  $E(S)|_{\mathbf{q}}$  for any desired value of  $S$ . When normalized to the same deformation point, the curves  $E(\mathbf{q})|_S$  and  $F(\mathbf{q})|_T$  should be strictly equivalent within the interpolation errors. This is verified in figure 1, where all dashed lines are obtained for the values of entropy at the top of the first barrier.

### 3.2. Temperature of the fragments

Until now, macroscopic-microscopic approaches assumed either the same temperature in the two fragments [15], or a ratio of temperatures proportional to the ratio of the fragment masses  $T_1/T_2 \approx A_1/A_2$  [16]. The validity of the Maxwell thermodynamical relations in a practical case suggests a method to predict microscopically the nuclear temperature of each individual fragment after scission.

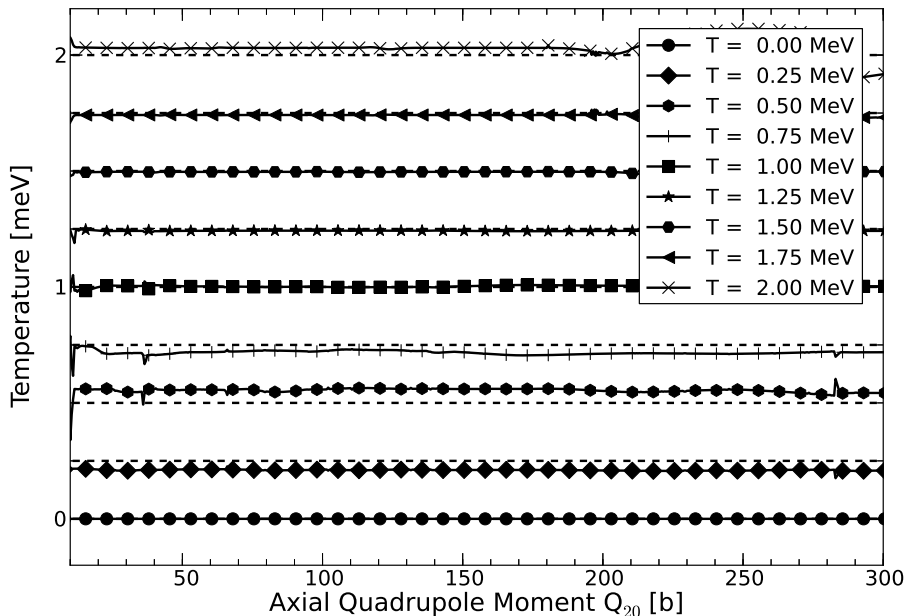


**Figure 2.** Temperature along the most probable fission path of  $^{240}\text{Pu}$  as extracted from the entropy as function of the internal energy.

As seen in the previous section, the isothermal and isentropic representations are equivalent. The advantage of the latter is that it involves only extensive variables, and is, therefore, more amenable to the description of the splitting of the compound nucleus into two subsystems. The scission of the compound nucleus, characterized with an internal energy  $E$  and an entropy  $S$ , yields two fragments, with respective internal energy and entropy  $(E_1, S_1)$  and  $(E_2, S_2)$ . Since the entropy is an extensive variable, we have  $S = S_1 + S_2$  (here, we have to assume implicitly that the interaction energy between the two fragments is ‘small enough’). The next step is to take advantage of the thermodynamical relation

$$\left. \frac{\partial S}{\partial E} \right|_{q_i} = \frac{1}{T}. \quad (2)$$

For each fragment  $n = 1, 2$ , we can perform a separate FT-HFB calculation constrained on the deformations  $q_i^{(n)}$  of the fragment at scission. This gives us the functions  $S^{(n)}(E^{(n)})$ . Taking the derivative with respect to  $E^{(n)}$  gives the temperature  $T^{(n)}$  of the fragment  $n$ . While the value of both the internal energy and entropy in this separate FT-HFB calculation should be the same as the ones extracted from the compound nucleus (again: if the interaction energy can be neglected), the temperature may be different, as it is related to the derivative  $\partial S/\partial E$ .

The method just outlined will be applied to estimating the temperatures of the fragments in the induced fission of  $^{240}\text{Pu}$  in a forthcoming publication. As a preliminary step, we estimate in figure 2 its numerical accuracy by comparing the exact value of the temperature, as set in the FT-HFB calculation, with the numerical estimates obtained from the  $S(E)$  function. Overall, the accuracy is of the order of 50 keV at worse, owing to interpolation errors.

#### 4. Conclusions

Recent advances in the nuclear energy density functional theory, combined with the constant increase of computing power, have enabled significant progress toward the development of a microscopic theory of nuclear fission. In this short article, we have presented early results related to the evolution of fission barriers with nuclear temperature and the equivalence between isentropic and isothermal representations.

#### Acknowledgments

Enlightening discussions with W. Younes and D. Gogny are very warmly acknowledged. This work was supported by the U.S. Department of Energy under Contract Nos. DE-AC52-07NA27344 (Lawrence Livermore National Laboratory) and de-sc0008499 (NUCLEI SciDAC Collaboration). An award of computer time was provided by the Innovative and Novel Computational Impact on Theory and Experiment (INCITE) program. This research used resources of the Oak Ridge Leadership Computing Facility located in the Oak Ridge National Laboratory, which is supported by the Office of Science of the Department of Energy under Contract DE-AC05-00OR22725. It was also supported by the National Energy Research Scientific Computing Center supported by the Office of Science of the US Department of Energy under Contract No. DE-AC02-05CH11231.

#### References

- [1] Berger J-F, Girod M and Gogny D 1984 *Nucl. Phys. A* **428** 23c
- [2] Berger J-F, Girod M and Gogny D 1989 *Nucl. Phys. A* **502** 85c
- [3] Bender M, Heenen P-H and Reinhard P-G 2003 *Rev. Mod. Phys.* **75** 121
- [4] Goutte H, Berger J F, Casoli P and Gogny D 2005 *Phys. Rev. C* **71** 024316
- [5] <http://computingnuclei.org>.
- [6] Kortelainen M, McDonnell J, Nazarewicz W, Reinhard P-G, Sarich J, Schunck N, Stoitsov M and Wild S M 2012 *Phys. Rev. C* **85** 024304
- [7] Younes W and Gogny D 2011 *Phys. Rev. Lett.* **107** 132501
- [8] Perlińska E, Rohoziński S G, Dobaczewski J and Nazarewicz W 2004 *Phys. Rev. C* **69** 014316
- [9] Dobaczewski J, Nazarewicz W and Stoitsov M 2002 *Eur. Phys. J. A* **15** 21
- [10] Goodman A L 1981 *Nucl. Phys. A* **352** 30
- [11] Bartel J, Quentin P, Brack M, Guet C and Håkansson H-B 1982 *Nucl. Phys. A* **386** 79
- [12] Stoitsov M, Schunck N, Kortelainen M, Michel N, Nam H A, Sarich J and Wild S 2012 *Preprint nucl-th/1210.1825*
- [13] Schunck N, Dobaczewski J, McDonnell J, Satuła W, Sheikh J A, Staszczak A, Stoitsov M and Toivanen P 2012 *Comp. Phys. Comm.* **183** 166
- [14] Pei J C, Nazarewicz W, Sheikh J A and Kerman A K 2009 *Phys. Rev. Lett.* **102** 192501
- [15] Wilkins B D, Steinberg E P and Chasman R R 1976 *Phys. Rev. C* **14** 1832
- [16] Schmidt K H and Jurado B 2010 *Phys. Rev. Lett.* **104** 212501